

# SiO<sub>2</sub>-P<sub>2</sub>O<sub>5</sub> THIN-FILM HUMIDITY SENSOR: METROLOGICAL CHARACTERIZATION

P. Arpaia<sup>(1)</sup>, M. D'Apuzzo<sup>(1)</sup>, S. Esposito<sup>(2)</sup>, R. Schiano Lo Moriello<sup>(1)</sup>

Università di Napoli Federico II, Polo delle Scienze e delle Tecnologie,

<sup>(1)</sup> Dipartimento di Ingegneria Elettrica, Via Claudio 21, 80125 Napoli,

Ph: ++ 39 081 7683238 - Fax. ++ 39 081 2396897, dapuzzo@unina.it

<sup>(2)</sup> Dipartimento di Ingegneria dei Materiali e della Produzione,

Piazzale Tecchio, 80125 Napoli, Ph: ++ 39 081 7682411, serena@unina.it

ITALY

**Abstract** – *A prototype of humidity sensor, based on a sol-gel ceramic compound of phosphorous pentoxide P<sub>2</sub>O<sub>5</sub> and silica SiO<sub>2</sub>, is presented. The sensing principle is based on the high affinity between phosphorous pentoxide and water: the frequency spectrum of the electrical impedance varies according to humidity with remarkable sensitivity. The silica basis allows the sensing element to be deposited on an oxidized silicon chip substrate for microsensor applications. The sol-gel production allows the sensing element to be easily developed as thin-film for fast time response. Design criteria and preparation procedure of the material, metrological characterization of the sensing element, and preliminary response tests of the sensor prototype are reported. Experimental results show the sensing element to be promising for a high-sensitive humidity low-temperature microsensor.*

**Keywords** - Humidity, Ceramic, Sol-Gel, Thin-film, Microsensor.

## 1. INTRODUCTION

Recent literature points out the ceramics as among the most promising materials for humidity sensing [1-3]. They are characterized by high thermal and mechanical resistance, as well as by strong chemical stability [4]. However, ceramic traditional realizing technologies, such as sinterization needing for a very-high pressure, are not suitable for thin-film production, necessary for reduced time response [5]. Conversely, new deposition technology, such as sol-gel, showed to have considerable potential: in particular, a high humidity sensitivity of phosphorous ceramic sol-gel compounds was pointed out. However, this was combined to a very low chemical stability and to the difficulty of realizing the material as a thin film [6-7]. Moreover, in thin-film production of on-chip integrated smart micro-transducers, problems of adhesion between the chip oxidized silicon substrate and the sensing material arise.

In this paper, a high-sensitive humidity sensing element, based on a sol-gel ceramic compound (phosphorous

pentoxide P<sub>2</sub>O<sub>5</sub> and silica SiO<sub>2</sub>), promising for low-temperature microsensor applications, is presented. The sensing principle is based on the high affinity between phosphorous pentoxide and water: the frequency spectrum of the electrical impedance varies according to the humidity with remarkable sensitivity. On the other hand, the silica basis allows the sensing element to be deposited on a silicon substrate with satisfying chemical stability. Moreover, the sol-gel production allows the sensing element to be easily produced as thin-film. In particular, in Section 2, the main criteria for the material design and the procedure for the sensing element preparation are outlined. In Section 3, experimental results of static metrological characterization of the sensing element are discussed. Finally, in Section 4, preliminary results of the impedance frequency response of the sensor prototype are shown.

## 2. THE SENSING ELEMENT

In the following, the *material design criteria* and the *preparation procedure* of the proposed sensing element are briefly recalled [8].

The *material design criteria* were aimed at satisfying the main microsensor requirements for low-temperature applications: (i) high sensitivity to humidity, i.e. affinity to water molecule, (ii) reduced response time, i.e. thin-film structure, and (iii) on-chip integrability, i.e. possibility of deposition on chip oxidized silicon.

These design problems have been faced by the sol-gel production of an inorganic material based on silica (SiO<sub>2</sub>) and phosphorous pentoxide (P<sub>2</sub>O<sub>5</sub>) [8]. In fact, the strong water affinity of the phosphorous pentoxide P<sub>2</sub>O<sub>5</sub> ensures high humidity sensitivity to the system: the reacting water causes the modulus and phase spectra of the material impedance to vary according to its amount. The silica SiO<sub>2</sub> ensures high chemical stability and allows easy deposition on a substrate suitable for microsensors such as oxidized silicon. Phosphorylchloride POCl<sub>3</sub> and tetraethoxysilane Si(OC<sub>2</sub>H<sub>5</sub>)<sub>4</sub> were used as starting materials in a sol-gel preparation suitable for thin-film ceramic element production. In particular, among the various investigated

Table I – Experimental plan CCRD for calibration.

| Exp. | T (°C) | R.H. (%) |
|------|--------|----------|
| 1    | 11.46  | 54.40    |
| 2    | 15.00  | 50.00    |
| 3    | 10.00  | 65.00    |
| 4    | 18.54  | 54.40    |
| 5    | 11.46  | 75.60    |
| 6    | 18.54  | 75.60    |
| 7    | 20.00  | 65.00    |
| 8    | 15.00  | 80.00    |
| 9    | 15.00  | 65.00    |
| 10   | 15.00  | 65.00    |
| 11   | 15.00  | 65.00    |
| 12   | 15.00  | 65.00    |
| 13   | 15.00  | 65.00    |

compositions of phosphosilicate solutions, the optimum trade-off was SiO<sub>2</sub> 70 % mol and P<sub>2</sub>O<sub>5</sub> 30 % mol [8].

The *preparation procedure* of the sensing element was set up iteratively by thermal and structural experimental analysis, carried out on dried and heat treated samples by DTA, FTIR, and NMR analytical techniques [8-10]. The resulting preparation procedure consists of the following steps:

1. A microscope glass is dip-coated into the solution and pulled out at 150 mm/min speed in order to produce a thin-film sensing element of thickness in the range from 0.8 to 1.0 μm;
2. The sensing element is dried in a electrical oven at 100 °C for a day;
3. It is stabilized by heating in the oven up to 300 °C at the rate of 2°C/min, and then cooled in air;
4. Two straight 5-mm distant electrodes are laid down on the element surface by a silver conducting paint in order to define the measuring points of the electrical impedance;
5. The sensing element is provided by a metallic shield to reduce random parasitic effects.

### 3. EXPERIMENTAL RESULTS OF METROLOGICAL CHARACTERIZATION

The metrological characterization was aimed at surveying the sensing element response in terms of: (i) *calibration*, i.e. frequency spectra of real and imaginary impedance parts as a function of static humidity and the main influencing parameters, such as the temperature; (ii) *repeatability*, i.e. frequency spectra of real and imaginary impedance parts as a function of humidity, in fixed measurement conditions; and (iii) *static hysteresis*, i.e. frequency spectra of real and imaginary impedance parts for quasi-statically increasing and decreasing humidity.

The analysis was carried out at the laboratory SIT (Italian Calibration Service) of the University of Cassino by means of a thermo-hygro-metric chamber WUG mod. ABDT/20JU, and a digital impedance meter Quadtech mod. 7600, specifically calibrated to operate in high-impedance range. Suitable measuring currents for the instrument were

achieved by a selecting a test sinewave rms of 1.0 V. Polarization and residual parasitic phenomena in the sensing element were made negligible by testing 25 points equally-spaced in log scale over the frequency range from 0.15 to 100 kHz. The ranges from 10 to 20 °C for temperature and from 50 to 80 % R.H were investigated preliminarily in order to assess performance of the sensing element in general-purpose applications.

#### 3.1 Calibration

In calibration experiments, the sensing element impedance, in terms of frequency spectra of real and imaginary parts, as a function of relative humidity (R.H.) and the main influencing parameters, such as temperature (T), was measured. The experimental burden was optimized in relation to the desired uncertainty in impedance estimate by statistical experiment design. Lack of a-priori information about the sensing element response to R.H. and T suggested the preliminary selection of (i) a second-order model for both the bidimensional relations of modulus and phase of impedance versus R.H. and T, in order to appreciate the response curvature at least, and (ii) a statistical plan Central Composite Rotatable Design (CCRD) for the experiments [11-12], in order to map the bidimensional test domain (R.H.,T) symmetrically and radially (Tab.I). For each experiment of the matrix, the frequency spectra of impedance modulus and phase were measured at the values of R.H. and T reported in the corresponding row of the matrix. Averages on 30 independent measurements were performed in order to filter the null-mean effects of other random influence parameters.

Then, bidimensional second-order response surfaces for both modulus and phase were obtained at varying frequency by statistical regression techniques [13]. An example of the obtained response surfaces for the impedance modulus is shown in Fig. 1, for the frequency best case in relative humidity sensitivity of 150 Hz. A satisfying sensitivity to humidity can be noted, in the temperature range as a whole. Conversely, very high values

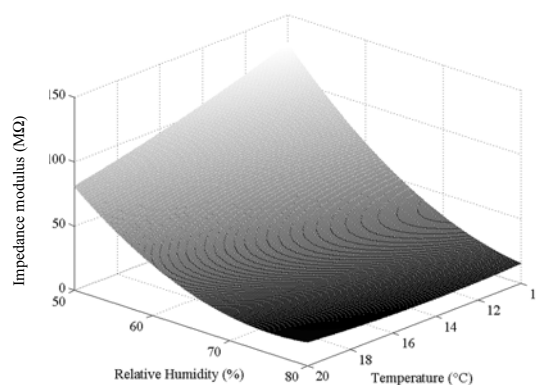


Fig.1 – Impedance modulus response surface of the sensing element (150 Hz).

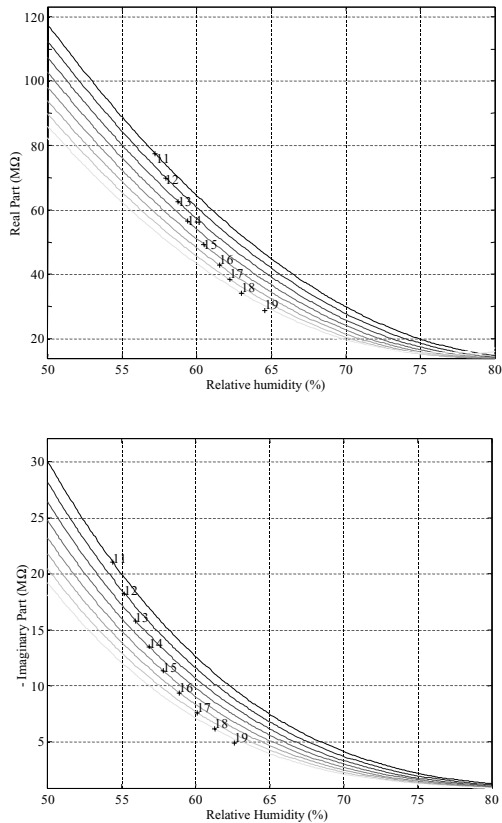


Fig.2 – Static calibration curves of the impedance real (upper) and imaginary (lower) parts, for temperature range from 10 to 20 °C (150 Hz).

of impedance modulus can be argued.

Examples of the obtained calibration diagrams are shown in Fig. 2, again for the sensitivity best case of 150 Hz: in particular, the trends of impedance real (upper) and imaginary (lower) parts versus relative humidity, at varying the temperature in the range from 10 to 20 °C, are reported. The relevant sensitivity to R.H. is confirmed, but joined also to a sensitivity to the temperature: it acts as the main influence parameter in the above range from 10 to 20 °C.

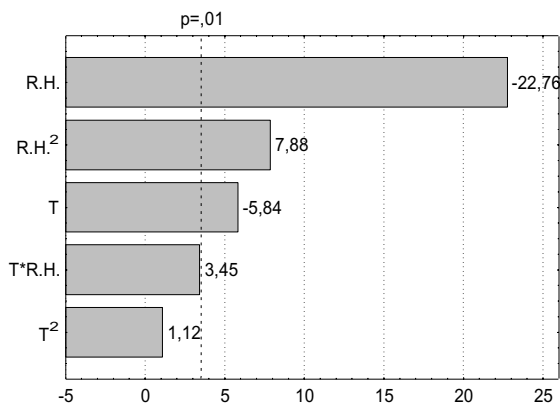


Fig.3 –Pareto charts of model terms ( $p=0.1$ : 99% significance level).

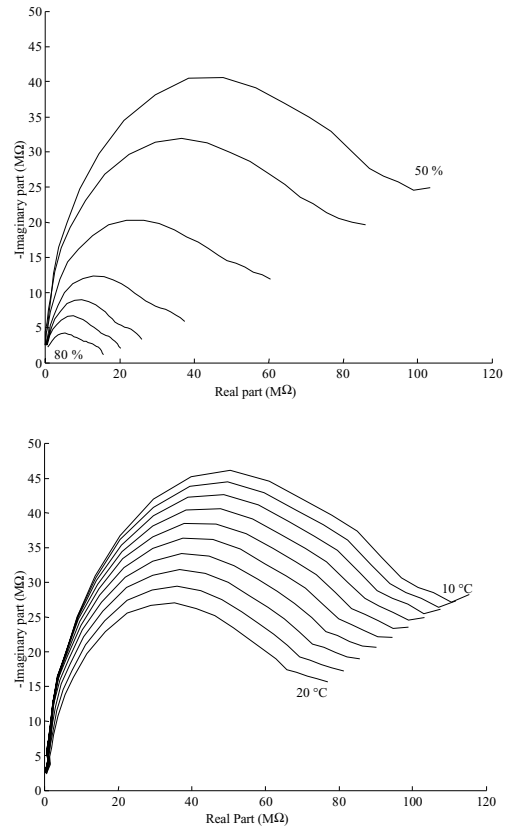


Fig. 4 – Static Nyquist diagrams, in the range from 0.150 to 100 kHz, at  $T=10$  °C (upper) and RH 50% (lower).

The statistical significance of the regression analysis was verified through the analysis of variance (ANOVA) [13]. A typical example of the Pareto chart [13] of the second-order model terms is reported for the modulus at 150 Hz in Fig.3. The significance (99% level) of the humidity (squared and linear R.H. terms) and of the temperature (linear terms) can be verified.

A further interesting result is the statistical independence of temperature and humidity: the trend shows that the cross term  $T \cdot R.H.$  is negligible at the above significance level of 99%. Analogous behaviors arose from all the 50 processed models over the frequency range as a whole for both the modulus and the phase of the impedance. This highlights a prospective usefulness of the proposed sensing element for a thermo-hygro-metric multiple sensor [14-15].

The sensitivity turns out to be satisfactory for both the factors T and R.H. in the investigated experimental plan as a whole (though the temperature sensitivity decreases at high relative humidity values). In the upper Nyquist plot of Fig. 4, an example of the sensitivity to the relative humidity, also for the lowest temperature of 10 °C is shown, though high values of impedance can be again appreciated. This makes the sensing element promising for freezing environment applications, once the impedance

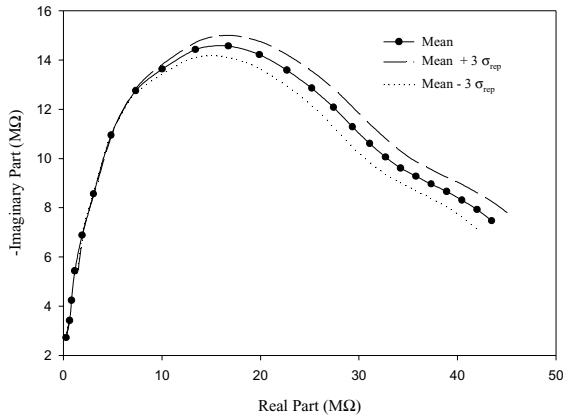


Fig.5 – Nyquist diagrams for repeatability ( $\sigma_{rep}$ : standard deviation).

values have been reduced in sensor engineering [16]. By increasing humidity (plots from 70 to 80 %R.H. in Fig.4 upper), the beginning of a second semicircle appears on the plots, owing to the capillary condensation phenomenon, causing a dielectric constant at lower frequency. In the lower Nyquist plot of Fig. 4, an example of the sensitivity to the temperature (R.H.=50%) over the most part of the investigated frequency range is shown.

It is worth to be remarked that, for each couple of humidity and temperature values, the spectroscopic technique produces results of real and imaginary impedance parts at several frequency points. This redundancy in information allows the measurement error to be minimized by means of suitable neural-based correction algorithms [17].

### 3.2 Repeatability

The repeatability of the sensing element versus relative humidity and temperature was investigated by carrying out 30 consecutive independent measurements of impedance spectrum at constant temperature and in the same test conditions. Fig. 5 shows an example of a typical trend for

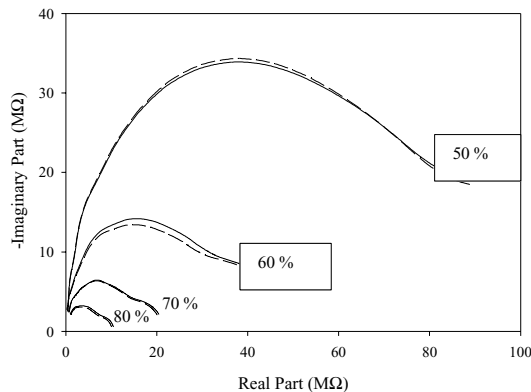


Fig.6 – Static hysteresis plots at 20 °C temperature (continuous and dashed lines: rising and falling test, respectively).

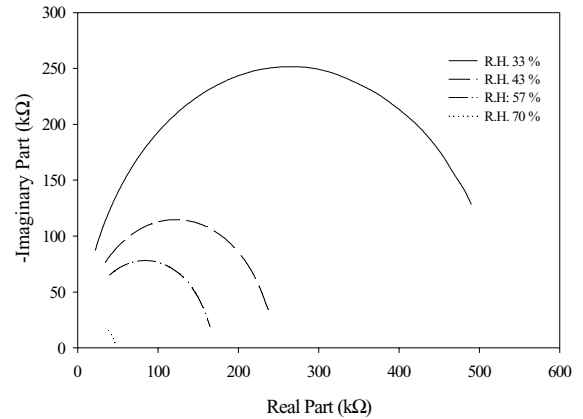


Fig.7 – Static preliminary characterization of the sensor prototype at 20 °C

$T=10\text{ }^{\circ}\text{C}$  and  $R.H.=65\%$ : the limit curves were obtained by enveloping rectangles having as sides 3-times the standard deviation of repeatability for both real and imaginary parts. A worst value of 3 % for repeatability over all the humidity ranges and temperature was detected.

### 3.3 Static Hysteresis

The static hysteresis was analyzed by measuring the element impedance for quasi-statically increasing and decreasing relative humidity. Fig. 6 shows an example of the resulting Nyquist plots at 20 °C in the range from 50 to 80 %: the couple of plots obtained for increasing (continuous lines) and decreasing (dashed lines) R.H. values are compatible by considering the corresponding uncertainty bands. The results showed the static hysteresis to be negligible over the investigated domain as a whole.

## 4. THE SENSOR PROTOTYPE

The preliminary static metrological characterization highlighted the main drawback for the sensing element material: an intrinsic too high impedance. In the sensor prototyping, this problem was faced by a suitable electrodes scheme: an interlocking combs geometry, based on a photolithographic deposition of Nb on Corning glass substrate, was realized. As well known, this electrode configuration, electrically working as several parallel circuits, allows a significant reduction of the sensor impedance [16].

An example of preliminary characterization result of the sensor prototype at  $T=20^{\circ}\text{C}$  is shown in Fig.7. By comparing these responses with the ones of Fig.4 (upper), a significant decrease in the prototype impedance can be observed (more than 2 magnitude orders), in spite of a still high sensitivity to humidity. A 200 mV rms voltage test signal was used, due to the reduced impedance value. Also a different frequency range from 20 to 500 kHz was tested, since the electrode arc circle due to polarization phenomena appears at higher frequency, owing to the different electrode metal and configuration.

## 5. CONCLUSIONS

The sensing element of a thin-film high-sensitive humidity ceramic sensor, suitable for low-temperature microsensor applications has been proposed. Preliminary experimental results of the static metrological characterization showed the sensing element satisfactory behavior in terms of sensitivity, repeatability, and hysteresis. Moreover, an independent sensitivity to relative humidity and temperature showed promising performance for multiple sensor.

At to date, further tests are ongoing aimed at investigating the dynamic behavior of the sensor prototype, especially in more critical low temperature and relative humidity ranges.

## ACKNOWLEDGMENTS

The work was supported on behalf of National Research Council of Italy (CNR), Targeted Project "Special Materials for Advanced Technologies II" (No. 980014 PF34).

## REFERENCES

- [1] Wu Huadong, M. Siegel, "Odor-based incontinence sensor", *Proc. of 17<sup>th</sup> IEEE IMTC 2000*, Baltimore, Vol.1, May 2000, pp. 63 – 68.
- [2] Don-Hee Lee et al., "A micromachined robust humidity sensor for harsh environment applications", *Proc. of 14<sup>th</sup> MEMS 2001*, 20001, pp.558–561.
- [3] P. Wiederhold, *Water Vapour Measurement: Methods and Instrumentation*, Dekker, New York, 1997.
- [4] E. Traversa, "Ceramic sensors for humidity detection: the state of the art and future developments", *Sens. and Act. B*, No. 23, 1995, pp. 135-156.
- [5] G. Neri et al., "Humidity sensing properties of Li-iron oxide based thin films", *Sens. and Act. B*, No. 73, Vol. 2-3, 2001, pp. 89-94.
- [6] N. Nogami, C. Wang, Y. Abe, "Fast proton conducting P<sub>2</sub>O<sub>5</sub>-SiO<sub>2</sub> glasses" *Proc. of XVIII Congr. on Glass*, Amer. Ceram. Soc., S. Francisco, 1998, Vol. D3, pp. 139-144.
- [7] Y. Abe et al., "Super-protonic conductor of glassy zirconium phosphates", *J. of Electrochem. Soc.*, Vol. 143, 1996, pp.144-149.
- [8] M. D'Apuzzo, A. Aronne, S. Esposito, P. Pernice, "Sol-gel synthesis of humidity-sensitive P<sub>2</sub>O<sub>5</sub>-SiO<sub>2</sub> amorphous films". *J. Sol-Gel. Sci. Tech.*, Vol. 17, 2000, pp. 247-254.
- [9] F. Settle, *Instrumental Techniques for Analytical Chemistry*, Prentice Hall, New Jersey 1997.
- [10] N. J. Clayden, S. Esposito, P. Pernice, A. Aronne, "Solid state <sup>29</sup>Si and <sup>31</sup>P NMR study of gel derived phosphosilicate glasses", *J. Mat. Chem.*, Vol. 11, 2001, pp.936-943.
- [11] W. J. Diamond, *Practical Experiment Design for Engineers and Scientists*, Lifetime Learning Publications, California, 1981.
- [12] P.Arpaia, *Experiment Design*, (In Italian), in N. Polese, *Measurements for the Management*, Edizioni Scientifiche Italiane, Rome, 2000.
- [13] D.C. Montgomery, *Design and Analysis of Experiments*, John Wiley & Son, New York, 1997.
- [14] J. Brignell, N. White, *Intelligent Sensor Systems*, Institute of Physics Publishing, Bristol and Philadelphia, 1996.
- [15] L. Michaeli, P. Kalakaj, A. Sak, M. Somora, *Korrektursystem für Temperatureinflüsse*, (In German), *Multisensorik Praxis*, Ch. 12, Ed. Horst Ahlers, Springer Verlag, Munchen, Berlin, 1996, p.211-219.
- [16] H. N. Norton, *Handbook of Transducers*, Prentice Hall, 1989.
- [17] P. Arpaia, P. Daponte, D. Grimaldi, L. Michaeli, "ANN-based error reduction for experimentally modeled sensors", *Proc. of IEEE IMTC-2000*, Baltimore, May, 2000, pp-1487-1492.